PAPER

Check for updates

Solvent-driven isomerization of *cis,cis*-muconic acid for the production of specialty and performance-advantaged cyclic biobased monomers†

Jack M. Carraher, [ID] ‡[a,b] Prerana Carter, [ID] ‡[a,b] Radhika G. Rao, [ID] [a,b]
Michael J. Forrester, [ID] [a] Toni Pfennig, [ID] [a,b] Brent H. Shanks, [ID] [a,b]
Eric W. Cochran [ID] [a] and Jean-Philippe Tessonnier [ID] *[a,b]

The quest for green plastics calls for new routes to aromatic monomers using biomass as a feedstock. Suitable feedstock molecules and conversion pathways have already been identified for several commodity aromatics through retrosynthetic analysis. However, this approach suffers from some limitations as it targets a single molecule at a time. A more impactful approach would be to target biopriviliged molecules that are intermediates to an array of commodity and specialty chemicals along with novel compounds. Muconic acid (MA) has recently been identified as a biopriviliged intermediate as it gives access to valuable aliphatic and cyclic diacid monomers including terephthalic acid (TPA), 1,4-cyclohexanedicarboxylic acid (CHDA), and novel monounsaturated 1,4-cyclohexenedicarboxylic acids (CH1DA, CH2DA). However, accessing these cyclic monomers from MA requires to first isomerize biologically-produced *cis,cis*-MA to Diels−Alder active *trans,trans*-MA. A major impediment in this isomerization is the irreversible ring closing of MA to produce lactones. Herein, we demonstrate a green solvent-mediated isomerization using dimethyl sulfoxide and water. The mechanistic understanding achieved here elucidates the role of low concentrations of water in reducing the acidity of the system, thereby preventing the formation of lactones and improving the selectivity to *trans,trans*-MA from less than 5% to over 85%. Finally, a Diels−Alder reaction with *trans,trans*-MA is demonstrated with ethylene. The monounsaturated cyclic diacid obtained through this reaction (CH1DA) can be converted in a single step into TPA and CHDA, or can be directly copolymerized with adipic acid and hexamethylenediamine to tailor the thermal and mechanical properties of conventional Nylon 6,6.

Introduction

The polymer industry has become a key driver for the research and development of biorenewable chemicals due to end user appeal for green plastics.[1–4] For instance, biobased terephthalic acid (TPA) is receiving significant attention due to its central role in the production of polyethylene terephthalate (PET), a commodity polyester broadly used in bottling and packaging.[5–17] Other cyclic targets include specialty chemical 1,4-cyclohexanedicarboxylic acid (CHDA), which is gaining attention for tuning properties in polyesters while enhancing their sustainability.[18,19] The market size for these cyclic building blocks is currently valued at $60 billion and is expected to further grow at an annual rate of 5%.[20,21] Therefore, even a conservative 5% replacement by biobased drop-in chemicals represents tremendous opportunities for the emerging biorenewable chemical industry.

Technologies developed to access cyclic molecules from renewable feedstocks have largely used retrosynthesis strategies. In the case of biobased TPA production, research has primarily focused on renewable *p*-xylene as a drop-in replacement for catalytic oxidation in the AMOCO process.[6–8,13,22,23] An alternate route towards these cyclic diacids is through muconic acid (MA), an intermediate produced from either sugar or lignin using metabolically engineered yeasts and bacteria.[24–28] The latter approach is particularly attractive as

[a]Department of Chemical and Biological Engineering, Iowa State University, Ames, IA 50011, USA. E-mail: tesso@iastate.edu
[b]Center for Biorenewable Chemicals (CBiRC), Ames, IA 50011, USA
†Electronic supplementary information (ESI) available: NOESY NMR spectrum of MA in water, NMR spectra of biobased *cc*MA and *ct*MA, GPC, DSC, and DMA results of the synthesized polyamides, experimental method for the synthesis of biobased *cc*MA and 1,4-cyclohexanedicarboxylic acid. See DOI: 10.1039/d0gc02108c
‡These authors contributed equally to this work.
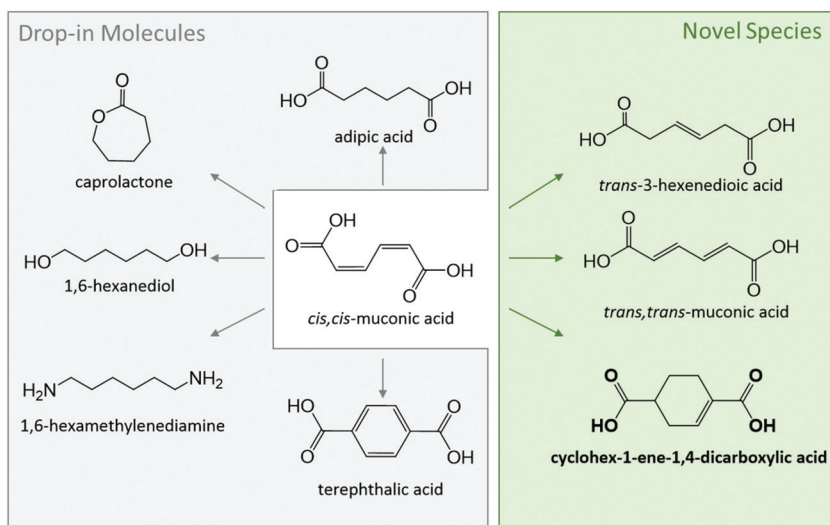
Scheme 1 Bioprivileged molecule *cc*MA produced biologically from sugar or lignin can be diversified into various drop-in and novel species.

MA is a bioprivileged molecule with substantial potential for diversification to commodity and specialty chemicals, as well as novel molecules for enhanced end-use properties (Scheme 1).[29–31] Previous work has already demonstrated the conversion of MA to an array of aliphatic commodity monomers including adipic acid and hexamethylenediamine,[24,25,32–36] cyclic monomers such as ε-caprolactam,[37,38] TPA and CHDA,[5,19,39,40] and novel mono-unsaturated compounds such as 3-hexenedioic acid and 1,4-cyclohex-1/2-enedicarboxylic acid (CH1DA, CH2DA).[19,41–44]

Although the downstream production of cyclic molecules has experienced some significant advances,[39,45] the initial isomerization of biologically-produced *cis,cis*-muconic acid (*cc*MA) to Diels–Alder active *trans,trans*-muconic acid (*tt*MA) remains a major bottleneck.[46] Only a handful of MA isomerization technologies have been reported in the literature. Notable ones use catalysts such as Pd/C (methanol reflux) or iodine either under UV light or in solvents such as tetrahydrofuran, methanol, or acetonitrile.[40,47–49] Various disadvantages, such as cost of noble metal catalysts, low selectivity, feed concentration limitations (*e.g.*, 10 wt% MA for the iodine system), hinder them from reaching the commercial realm.[5] The key obstacle in this seemingly simple isomerization is the spontaneous ring-closing of *cis,cis*- and *cis,trans*-MA (*ct*MA) to form the muconolactone (Mlac) and dilactone (Lac2). A previous report published by our group detailed the driving forces behind this lactonization when the isomerization is performed in water, and suggested several strategies to circumvent those driving forces.[19]

The present work investigates an organic solvent-mediated isomerization and demonstrates its clear potential to be scaled. It is shown here that the addition of water to the green aprotic solvent dimethyl sulfoxide (DMSO),[50,51] enhances selectivity to *tt*MA ($S_{tt\text{MA}}$) by 13-fold at 20% conversion. A comprehensive mechanistic understanding of the role of water was achieved through a series of reactions with *ct*MA in DMSO/

water solvent systems. As a proof of concept, *tt*MA was reacted with ethylene to produce the novel unsaturated molecule 1,4-cyclohex-1-enedicarboxylic acid (CH1DA); finally, a novel polyamide was formed through copolymerization with adipic acid and hexamethylenediamine. Overall, this study demonstrates a green, solvent-driven, scalable isomerization of MA in order to synthesize renewable cyclic diacids.

Results and discussion

While *cc*MA readily isomerizes to *ct*MA at room temperature,[19,52] further isomerization to Diels–Alder active *tt*MA is hindered by the intramolecular lactonization between unsaturated carbon–carbon and carboxylic acid moieties. We previously showed that the aprotic solvent DMSO impedes this lactonization and allows for high $S_{tt\text{MA}}$ (88%).[19] To investigate this conversion on a more industrially relevant scale, a sample with a *cc*MA concentration on the order of 300 g L^{-1} (~2 M concentration) was prepared in DMSO-d$_6$. Despite ^{1}H NMR spectra at such a high concentration being qualitative at best, heating a highly concentrated solution of *cc*MA at 100 °C overnight ($t_{\frac{1}{2}}$ ~ 2–4 hours) yielded primarily Mlac with no indication of the expected *tt*MA product. This result contrasted with our prior study,[19] indicating an effect of reactant concentration on the isomerization reaction. Therefore, this system was investigated kinetically in order to develop optimization strategies for the isomerization to *tt*MA.

Effect of muconic acid concentration in dry DMSO-d$_6$

The experiments in this study used *ct*MA as the starting material, with concentrations ranging from 5 to 80 mM. Reactions were typically performed at 87 °C unless stated otherwise. The product selectivity at 20% and 50% conversion was determined as a function of initial *ct*MA concentration ([*ct*MA]$_0$) as shown in Table 1 and Fig. 1. Maximum $S_{tt\text{MA}}$

Table 1 Effect of initial ctMA concentration on observed rate constants at 87 °C and product selectivity at 20% and 50% conversion

$[ctMA]_0$ (mM)	$k_{obs} \times 10^{6\ a}$ (s^{-1})	Half-life (days)	Selectivity (20% conversion)				Selectivity (50% conversion)			
			$ccMA$	$ttMA$	Mlac	Lac2	$ccMA$	$ttMA$	Mlac	Lac2
5.5	2.6	3.1	0.8%	19.0%	35.0%	37.3%	0.4%	14.6%	26.0%	31.0%
29.0	1.9	4.2	6.3%	12.0%	51.5%	25.0%	1.6%	6.4%	34.8%	34.2%
45.0	1.8	4.4	6.5%	6.3%	55.0%	26.0%	1.8%	4.0%	37.6%	35.6%
79.0	2.1	3.8	7.5%	3.0%	47.5%	15.0%	1.6%	3.0%	36.4%	32.4%

[a] k_{obs} was determined at low conversion (*ca.* 20%) from eqn (1). Error in k_{obs} was determined by least squares method to be $\pm 1 \times 10^{-7}$ s^{-1}.
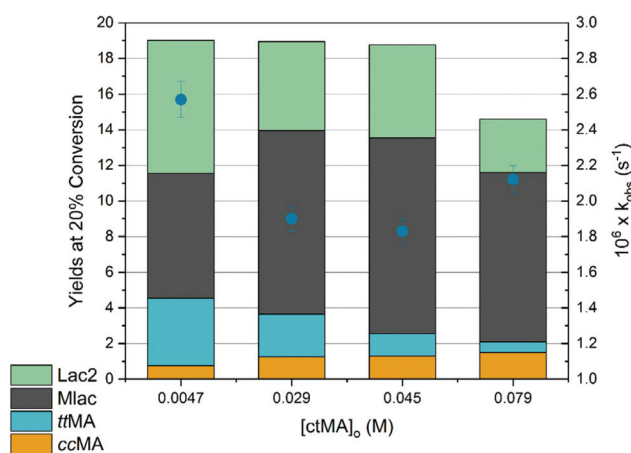

Fig. 1 Effect of $[ctMA]_0$ on yields at 20% conversion (left axis) and the observed rate constant (right axis). 5–80 mM ctMA solutions in DMSO-d_6 and heated to 87 °C. Kinetic traces and product distributions were obtained by ^{1}H NMR monitoring with $DMSO_2$ internal standard.

(19%) was observed at low conversion (*ca.* 20%) and the lowest $[ctMA]_0$. S_{ttMA} gradually decreased from 19% to 3% as $[ctMA]_0$ increased from 5 mM to 79 mM at 20% conversion. Additionally, S_{ttMA} at $[ctMA]_0$ of 5 mM decreased from 19% to roughly 15% as conversion increased from 20% to 50%. Several new signals consistent with MA degradation and formation of unidentified products were observed for all $[ctMA]_0$. This degradation was observed to occur more readily at elevated ctMA concentration. The significant drop in S_{ttMA} with increasing $[ctMA]_0$ suggests an acid catalyzed pathway for lactonization analogous to the aqueous system.[19] However, in this particular system, muconic acid is both the reactant and the catalyst as is shown in Scheme 2.
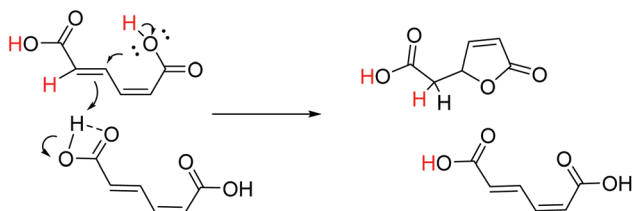
Scheme 2 Bimolecular pathway for muconic acid catalyzed lactonization scheme.

Kinetic traces obtained for the consumption of ctMA are consistent with a first order rate equation (eqn (1)) for all $[ctMA]_t$.

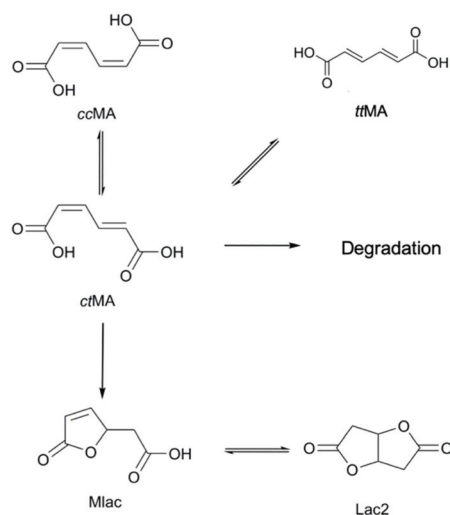$$\ln([ctMA]_t/[ctMA]_0) = -k_{obs} \times t + \text{const.} \qquad (1)$$

where $[ctMA]_t$ = concentration of ctMA at time t, $[ctMA]_0$ = initial concentration of ctMA, k_{obs} = observed first order rate constant, t = time in seconds, and const. = integration constant of first order rate law.

Fig. 1 shows the observed rate constants (k_{obs}) obtained from eqn (1) plotted against $[ctMA]_0$. The trend for k_{obs} with increasing $[ctMA]_0$ is somewhat peculiar and initially unexpected as the isomerization of ccMA and ctMA to ttMA was shown to be unimolecular in an aqueous system.[19] Therefore, an acid-catalyzed pathway that generates lactones would be expected to generate a linear plot with a *y*-intercept equal to the sum of all rate constants for unimolecular MA reactions and a slope corresponding to $k_{acid\text{-}catalysed}$ (M^{-1} s^{-1}). The unimolecular reaction pathways would include isomerization, unimolecular lactonization, and unimolecular degradation (Scheme 3). However, k_{obs} was found to initially decrease with increasing $[ctMA]_0$ between 5 and 45 mM and then increase between 45 and 79 mM. The initial decrease at low $[ctMA]_0$ suggested an equilibrium with a non-reactive species like an unreactive MA complex. Though kinetically observable, the non-reactive complex was not identifiable spectroscopically. At higher $[ctMA]_0$ the acid catalyzed pathway shown in Scheme 2 appeared to be dominant. In addition to higher Mlac yields, elevated $[ctMA]_0$ also resulted in significantly higher degradation to unidentified byproducts. Clearly, in the absence of water, this system is rather complex and will not offer high S_{ttMA} under industrially relevant conditions (*i.e.* high concentration). It was therefore decided to minimize efforts in this system and focus on approaches that take into consideration the effect of $[ctMA]_0$: (i) an acid-catalyzed lactonization pathway and (ii) the potential for reversible formation of a non-reactive complex/es. The former is more important as it clearly dominates near the solubility limit. It was therefore concluded that decreasing the apparent acidity should improve S_{ttMA}.

Effect of low water concentrations on muconic acid isomerization

The Dumesic group demonstrated that the addition of water to solid-acid catalyzed systems in DMSO and γ-valerolactone

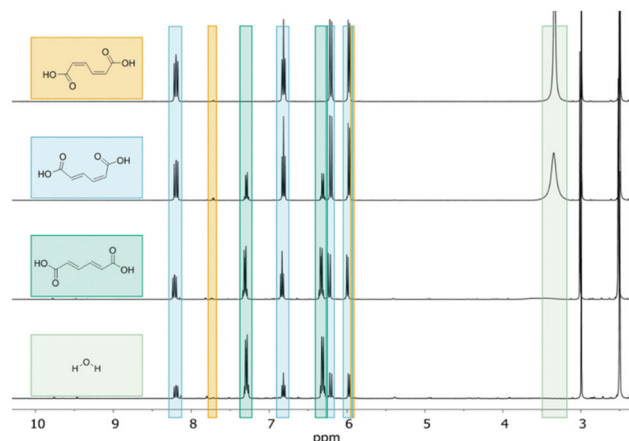**Scheme 3** Unimolecular reaction pathways for ctMA.

Fig. 2 ^{1}H NMR (600 MHz, DMSO-d_6) spectra of 48 mM ctMA + 96 mM H_2O heated to 87 °C at 0 (top), 18.5, 52, and 72.5% (bottom) conversion.

(GVL) can significantly decrease the activity of the catalyst.[53] The decrease in catalyst activity could be attributed to a more widespread hydrogen bonding network near the active sites, which effectively decreases their pK_a. This rationale was extended to our reaction system by introducing water to minimize the acid-catalyzed lactonization of ctMA. The experiments in this section were carried out using 48 mM ctMA in dry DMSO-d_6 with varying concentrations of water ([H_2O]). ^{1}H NMR spectra of samples containing water (5 mM–744 mM) indicated that MA was in its fully protonated (ctMAH$_2$) form under all conditions.

At very low [H_2O] the reactivity of ctMA was similar to that of the dry DMSO system at 20% conversion (compare 45 mM ctMA in Table 1 with 5 mM H_2O in Table 2). S_{ttMA} at 96 mM H_2O (H_2O : MA ~ 2 : 1) increased 13-fold to 81.5% (88% if conversion is considered as conv. = [ctMA]$_0$ − ([ctMA]$_t$ + [ccMA]$_t$)/ [ctMA]$_0$ due to the relatively rapid ccMA ↔ ctMA equilibrium). For [H_2O] of 96 mM, high S_{ttMA} (82%) was maintained up to 50%

conversion. Additionally, throughout this reaction the ^{1}H NMR signal of H_2O (3.34 ppm) gradually decreased with increase in conversion as shown in Fig. 2, until it was not observable after 52% conversion. The majority of the samples showed an increased S_{ttMA} with decreasing H_2O signal, suggesting that an optimal ratio of H_2O : MA exists for a highly selective production of ttMA (≥75%). This optimal range appears to be broad, varying from a H_2O : MA ratio of 0.9 : 1 to 10 : 1.

Kinetically, the conversion of ctMA follows first order rate equations. As the water content was increased, there was an initial 20% drop in k_{obs} between 5 mM and 38 mM, followed by a gradual increase (70–120 mM H_2O), and a plateau from 120 mM to 744 mM. The initial decrease was expected under the assumption that an acid-catalyzed lactonization pathway exists in parallel to unimolecular isomerization, and that introduction of water to the system would decrease the apparent pK_a. The sigmoidal shape observed in Fig. 3 could be indicative of a ctMA-2H_2O complex that is roughly 20% more active for isomerization to ttMA than a ctMA-H_2O complex. The plateau achieved at high [H_2O] coupled with decreasing H_2O

Table 2 Effect of water concentration on muconic acid isomerization in DMSO[a]

[H_2O]$_0$ (mM)	$10^6 \times k_{obs}$[b] (s^{-1})	Half-life (days)	Selectivity at 20% conversion			Selectivity at 50% Conversion		
			ccMA	ttMA	Mlac	ccMA	ttMA	Mlac
5.0	1.8	4.5	6.5%	6.3%	55.0%[c]	1.8%	4.0%	37.6%
37.7	1.4	5.9	7.5%	70.0%	3.5%	1.8%	69.8%	2.8%
55.6	1.4	5.9	7.5%	75.0%	3.0%	1.8%	71.2%	2.8%
70.1	1.3	6.2	7.5%	77.5%	4.0%	1.9%	79.0%	2.7%
74.6	1.5	5.4	7.5%	76.0%	3.0%	1.8%	78.2%	2.6%
96.1	1.5	5.5	7.5%	81.5%	3.0%	1.8%	82.0%	2.6%
115.8	1.7	4.7	7.5%	80.0%	2.5%	1.8%	70.0%	2.4%
157.4	1.6	5.0	7.5%	80.0%	2.5%	1.8%	72.0%	2.2%
322.0	1.6	5.0	7.5%	75.0%	4.5%	2.1%	83.7%	2.5%
478.0	1.6	5.0	7.5%	75.0%	4.5%	2.4%	85.7%	2.4%
744.0	1.6	5.0	7.0%	70.0%	3.0%	2.4%	79.0%	2.4%

[a] Selectivities at 20 and 50% conversion for 48 mM ctMA in DMSO-d_6 with varying concentrations of water at 90 °C. [b] k_{obs} acquired from fits to eqn (1) at 20% ctMA conversion. [c] 5 mM H_2O sample also contains Lac2.
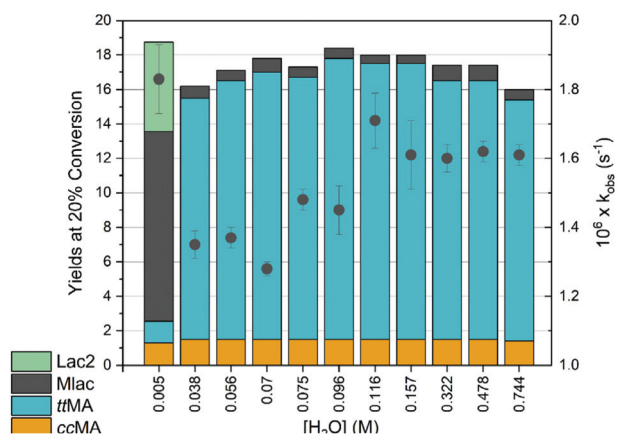
Fig. 3 Effect of water content on yields at 20% conversion (left axis) and the observed rate constant (right axis). Microliter amounts of water were added to 600 μl of 48.0 mM ctMA solutions in DMSO-d_6 and heated to 87 °C. Kinetic traces and product distributions were obtained by ^{1}H NMR monitoring with $DMSO_2$ internal standard.

signal and steady decline in S_{ttMA} above 160 mM H_2O could also be indicative of H_2O being a potential reactant in the degradation pathway.

Probing the effect of muconic acid at low water concentration

To probe the effect of $[ct$MA$]_0$ on the kinetics and yields at low water concentrations, these experiments were carried out with D_2O : MA of (1.9–2.6) : 1 ($[ct$MA$]_0$ ranging from 0.049–0.16 M). Under these conditions the water should interact primarily with the carboxyl moieties, lowering their apparent acidity and minimizing the acid-catalyzed lactonization shown in Scheme 2. This assumption is supported by NOESY NMR experiments showing proximity between the carboxyl moieties and H_2O in the system (ESI 1†). However, it should be noted that the NOESY spectrum is not definitive proof for the absence of H_2O association with internal carbon atoms.

The selectivity to cc- and ttMA at 20% conversion remained relatively constant between 50 and 160 mM ctMA ($ca.$ 6 and 75–80%, respectively), but selectivity to Mlac increased 6-fold (Fig. 4). Additionally, k_{obs} for ctMA consumption decreased with increasing $[ct$MA$]_0$, similar to that observed under dry DMSO. However, unlike the trend observed in Fig. 1, the rate constants did not increase again at higher $[ct$MA$]_0$. This observation supports the non-reactive complex hypothesis presented above.

Effect of high water concentrations on muconic acid isomerization

D_2O in concentrations ranging from 1.8 M to 16.0 M was added to a 50 mM ctMA solution resulting in a decrease in k_{obs} for ctMA consumption from 2.1×10^{-6} s^{-1} to 1.0×10^{-6} s^{-1}, as shown in Fig. 5. ttMA yields at 20% conversion remained relatively constant (15 ± 1%) up to 8.5 M D_2O but were halved to 7.5% at 16 M D_2O. This was accompanied by a slight decrease in equilibrium concentrations of ccMA and a 10-fold increase in Mlac yields (Fig. 5). Mlac yields rose steadily from 0.1% to 0.5% as $[D_2O]$ increased from 1.8 to 8.5 M, and then jumped to 5.5% at 16 M D_2O. Rate constants obtained by initial rates
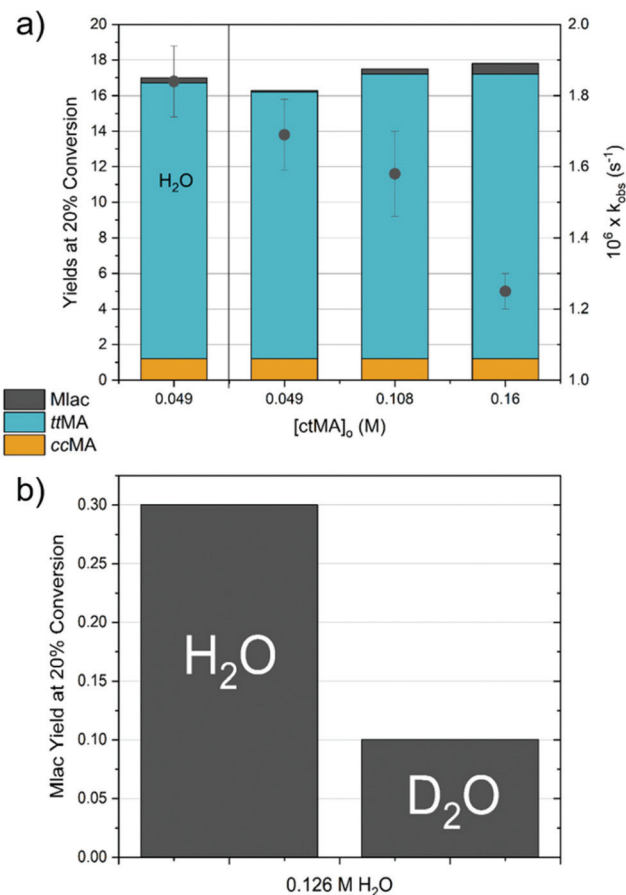

Fig. 4 (a) Effect of $[ct$MA$]_0$ with 2–2.6 equivalents of H_2O (column 1) and D_2O (columns 2–4) on yields at 20% conversion (left axis) and the observed rate constant (right axis) for ctMA solutions in DMSO-d_6 heated to 87 °C. Kinetic traces and product distributions were obtained by ^{1}H NMR monitoring with $DMSO_2$ internal standard. (b) Comparison of Mlac yield in H_2O and D_2O.

analysis for Mlac formation (eqn (2)) were plotted as a function of $[D_2O]$. The results suggested a ternary reaction in which water promotes lactonization through a push–pull type interaction, where one water molecule donates a proton to the δ carbon of the cis-carboxylic acid while another accepts the proton from the cis-carboxylic acid (Scheme 4). This observation is consistent with the large negative entropy of activation ($\Delta S^{\ddagger} = -110$ J (mol K)$^{-1}$) obtained from simulations fitted to experimental data for the same reaction in an aqueous system.[19] The rate constant for Mlac formation at 16 M D_2O obtained from eqn (2) is consistent with the aqueous simulations ($4 \pm 2 \times 10^{-7}$ s^{-1} at 16 M D_2O and 3×10^{-7} s^{-1} at 55 M).[19] This of course is only consistent if the reaction reaches kinetic saturation near 16 M D_2O (i.e. D_2O : ctMA = 320 : 1). The elementary rate constant for the ternary reaction shown in Scheme 4 was calculated to be $2 \pm 1 \times 10^{-9}$ M^{-2} s^{-1}.

$$\text{rate}_{\text{Mlac}} = [\text{Mlac}]_t / t \rightarrow k_{\text{Mlac}} = \text{rate}_{\text{Mlac}} / \{\frac{1}{2}([ct\text{MA}]_0 - [ct\text{MA}]_t)\}$$
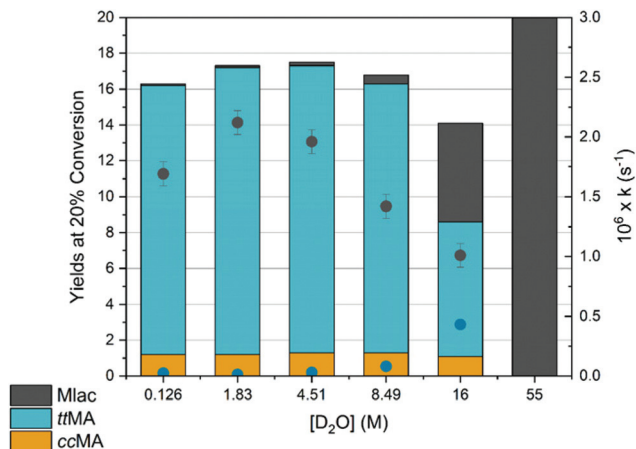
(2)

Fig. 5 Effect of high water content on yields at 20% conversion (left axis). The observed rate constant for *ct*MA conversion (black ●, right axis) was obtained from eqn (1) and the observed rate constant for Mlac formation (blue ●, right axis) was estimated from eqn (2). *ca.* 50 mM *ct*MA solutions in DMSO-d_6 + D_2O were heated to 87 °C. Kinetic traces and product distributions were obtained by ^1H NMR monitoring with $DMSO_2$ internal standard. The column at 55 M D_2O is from a previous experiment and the rate constant obtained is from simulations fit to experimental data in an aqueous system.[19]
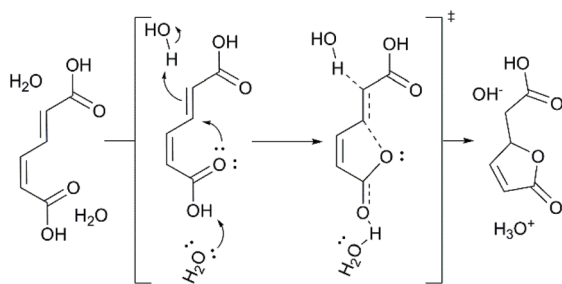
Scheme 4 Ternary lactonization process with *ct*MAH₂.

where [Mlac]$_t$ = Mlac concentration at time t, t = time in seconds at which ~5% *ct*MA conversion was achieved, k_{Mlac} = rate constant for the formation of Mlac, [ctMA]$_0$ = initial *ct*MA concentration, and [ctMA]$_t$ = concentration of *ct*MA at time t.

In addition to the solvent driven lactonization, higher water content also showed a decrease in the rate constant for *tt*MA formation. The rate constant k_{ttMA} was obtained by the same method as k_{Mlac} shown in eqn (2). These rate constants were relatively unaffected up to 8.5 M D_2O but decreased by nearly a factor of 5 from 8.5 to 16 M D_2O. At 16 M D_2O k_{ttMA} was roughly equivalent to k_{Mlac} whereas at 8.5 M D_2O k_{ttMA} = 84 × k_{Mlac}. The increase in k_{Mlac} with [D_2O] was expected for the reaction outlined in Scheme 4, however, the driving forces behind this significant decrease in k_{ttMA} were unclear. At 121 °C the *ct*MA to *tt*MA reaction was found to be reversible, *vide infra*. It is possible that water has an effect on the forward and/or reverse reaction(s). Therefore, the reactivity of 50 mM *tt*MA at 1.8 and 16 M D_2O was tested, which confirmed reversibility at 87 °C. Comparison of k_{obs} starting from both *ct*MA and *tt*MA yielded apparent equilibrium constants (K_{app}) that vary with [D_2O], K_{app} = 7.2 and 1.5 at 1.78 M and 16 M D_2O, respectively. The effect of water concentration on this equilibrium is exclusively a result of high water content slowing the forward reaction ($ct \rightarrow tt$) as the reverse reaction ($tt \rightarrow ct$) rate constant was the same at both 1.8 and 16 M D_2O (k_{tt-ct} = 3 ± 1 × 10^{-7} s^{-1}).

The solvent driven lactonization at high water concentration in conjunction with the significant decrease in k_{ttMA} at 16 M D_2O (neat D_2O = 55 M) would help explain why *tt*MA is never observed in an aqueous system in the absence of catalyst like La^{3+}.[19]

Effects of temperature & kinetic simulations

An investigation into the effects of temperature on the reaction system with *ca.* 2 equivalents of water was carried out. Product yields at 20% conversion and k_{obs} for *ct*MA conversion are shown in Fig. 6. S_{ttMA} was relatively high for all three temperatures; 88, 80, and 88% at 60, 87, and 121 °C, respectively (91, 88, and 93% considering the *cc*MA ↔ *ct*MA equilibrium). The reaction at 121 °C was fast enough ($t_{\frac{1}{2}}$ = 5.2 weeks, 5.2 days, and 1.7 hours at 60, 87, and 121 °C, respectively) that we were able to achieve equilibrium between *ct*MA and *tt*MA. While this is reasonable, it was surprising due to previous observations in which aged aqueous solutions of *tt*MA and *tt*MA in DMSO with no added water at 200 °C do not appear to yield *ct*MA. To probe the temperature effects further, kinetic simu-
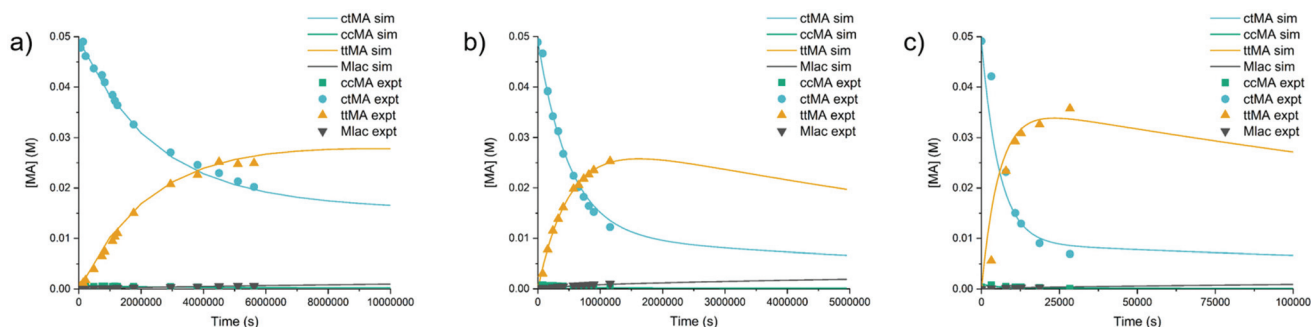

Fig. 6 Experimental (■) and simulated (—) traces of *ct*MA isomerization at 2 equivalents of D_2O at (a) 60 °C (b) 87 °C (c) 121 °C.

Table 3 Equilibrium constants, rate constants, and activation parameters for the reactions outlined in Scheme 4 [a]

Reaction	Temperature (°C)			Activation parameters[d]	
	60	87	121	$\Delta H^{\ddagger}$ kJ mol^{-1}	$\Delta S^{\ddagger}$ J (mol K)$^{-1}$
K_{cc-ct}[b]	68	55	50	—	—
K_{ct-tt}[b,c]	1.7	2.4	4.7	—	—
$k_{ct \to tt}$	2.5×10^{-7}	1.2×10^{-6}	1.4×10^{-4}	110 ± 31	-44 ± 85
$k_{tt \to ct}$	1.5×10^{-7}	5.0×10^{-7}	3.0×10^{-5}	92 ± 28	-103 ± 78
$k_{ct \to Mlac}$	4.0×10^{-9}	3.1×10^{-8}	6.0×10^{-6}	128 ± 31	-25 ± 86
$k_{ct \to deg}$	2.0×10^{-8}	3.5×10^{-7}	3.0×10^{-5}	128 ± 14	-11 ± 39

[a] All reactions were carried out in DMSO-d$_6$ with 1.9–2.5 equivalents of D$_2$O relative to 50 mM *ct*MA. [b] Equilibrium constants expressed with the subscript 'isomer1–isomer2' are for reversible isomerization and should not be confused with equilibrium constants with the subscript 'isomer1,isomer2' mentioned above as they represent K for formation of non-reactive complexes of the different isomers. [c] K_{ct-tt} is an apparent equilibrium constant derived from kinetic information about the forward and reverse reactions obtained from fitting the simulation to experimental values and does not represent the thermodynamic equilibrium. [d] Activation parameters are calculated for the reactions outlined in Scheme 3 and are specific to the system at 50 mM *ct*MA with 2 equivalents of H$_2$O. They do not take into consideration the equilibrium formation of potential non-reactive complexes.

lations were run with KINSIM software in accordance with the simplified Scheme 4. Estimates for elementary rate constants were input based on the experimental values obtained from treatment of the data with either eqn (1) or (2). The rate constants were finely tuned until simulated kinetic traces matched experimental ones for all species, including the loss of signal due to degradation from *ct*MA. The equilibrium constants, rate constants, and activation parameters are shown in Table 3. While the simulations starting from *ct*MA fit well with the experimentally obtained kinetic traces, simulating the reverse reaction (*e.g.* starting from *tt*MA) required decreasing k_{cc-tt} by a factor of 10.

Perhaps non-reactive complexes dependent upon [MA] exist for each of the isomers (see next section on *cc*MA). The equilibria achieved for these unreactive complexes will likely have equilibrium constants that are dependent upon the specific isomer pair. That is to say $K_{cc,cc}$ may be significantly different than $K_{ct,ct}$, $K_{tt,tt}$, $K_{cc,ct}$, $K_{cc,tt}$, and $K_{ct,tt}$. The focus of this investigation, however, is the unprecedented catalyst-free isomerization of *ct*MA to *tt*MA. Therefore, a more thorough study of these potential non-reactive complexes was not carried out at this time.

As a high $S_{tt\text{MA}}$ was achieved with 2 equivalents of D$_2$O at 121 °C (Fig. 6c), these conditions were selected to investigate the isomerization of *ct*MA under more industrially relevant conditions, namely at 70 and 300 g L^{-1} (*ca.* 0.5 and 2.0 M). In contrast to the experiment in dry DMSO-d$_6$ that prompted this study (*vide supra*), the reaction with 2.0 M *ct*MA and 2 equivalents of D$_2$O produced minute amounts of Mlac. However, the reaction quickly reached an equilibrium between *ct*MA and *tt*MA favoring *ct*MA (nearly 75 : 1 at 121 °C). This [*ct*MA]$_0$ effect was not observed at 70 g L^{-1} (~0.5 M), a concentration equivalent to the

Table 4 Rate constants for isomerization of *cc*MA[a]

[*cc*MA]$_0$ (mM)	[D$_2$O] (M)	$10^7 \times k_{obs}$ (s^{-1})
5	0.009	1.6
20	0.009	0.8
5	4.9	4.1
4	9.8	4.6
3	21.5	4.6

[a] Isomerization was carried out at 22 ± 1 °C in DMSO-d$_6$ and monitored by ^{1}H NMR. Selectivity to *ct*MA was 100% and signal loss due to degradation was not observed.

highest titers reported to date for biologically-produced *cc*MA. $S_{tt\text{MA}}$ reached 78% at 50% conversion, which is similar to the selectivity achieved with a 48 mM solution (Table 2).

Isomerization from *cis,cis*-muconic acid

As was the case with *ct*MA, ^{1}H NMR spectra obtained of solutions initially containing *cc*- and *tt*MA were consistent with the fully protonated form (MAH$_2$). These experiments are outlined in Table 4. Kinetic traces for the isomerization of *cc*MA to *ct*MA were fitted to 1st order rate equations with R^2 values ≥97%. Values for k_{obs} decreased with increasing [*cc*MA]$_0$ in the presence of 9 mM H$_2$O. This is consistent with the potential formation of a non-reactive MA complex and the lack of an acid catalyzed pathway for *cc*MA.[19] Addition of D$_2$O to the system increased k_{obs} implicating water as a non-innocent solvent consistent with the aqueous $\Delta S^{\ddagger} = -88$ J (mol K)$^{-1}$ for *cc*- to *ct*MA isomerization of MAH$_2$.[19] This effect appears to reach saturation at high H$_2$O : *cc*MA ratios. Unlike experiments in which *ct*MA was the initial isomer, no loss of signal was observed with reaction time, and selectivity to *ct*MA was 100%. This supports the above hypothesis that degradation of MA occurs from the *ct*-isomer.

Isomerization from biobased *cis,cis*-muconate

The robustness of the isomerization process, specifically its tolerance to impurities, was investigated using a fermentation broth containing 70 g L^{-1} (~0.5 M) of *cis,cis*-ammonium muconate (ESI†). The broth was first filtered over activated carbon to remove biogenic impurities and organic byproducts. *cc*MA was subsequently precipitated by acidification of the solution using 5 M sulfuric acid. The precipitate was recovered by filtration, rinsed with a minimum amount (10 ml) of 5 M sulfuric acid to prevent its redissolution, and dried overnight at room temperature. The biobased *cc*MA was then isomerized to *ct*MA using the procedure described previously. Further isomerization to *tt*MA was carried out in DMSO with 1.5 equivalents of H$_2$O. The *tt*MA yield at 50% conversion reached 34.8%, which is on par albeit lower than the yield obtained for reagent-grade *cc*MA (39.5%), see Fig. 7. This difference can be at least partly attributed to residual sulfuric acid that catalyzed the lactonization of *cc*MA during the isomerization step to *ct*MA, as indicated by ^{1}H NMR (ESI 2 and 3†). This issue could be easily addressed by improving the separation–purification process, which is beyond the scope of the present work.
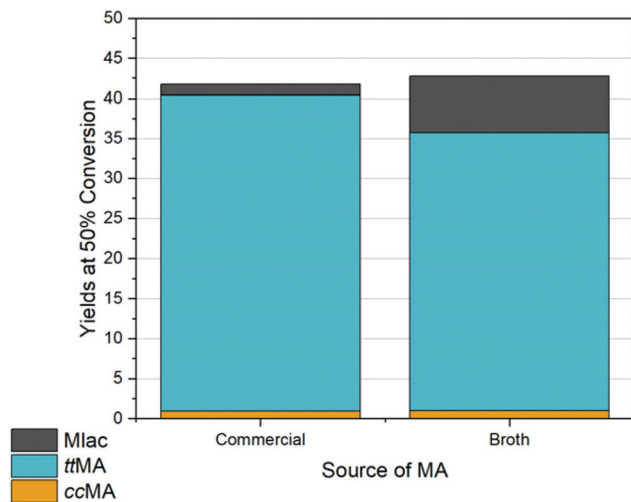
Green Chemistry

Paper

Fig. 7 Product distribution and yields obtained at 50% conversion when the reaction was carried out with reagent-grade ccMA and bio-based ccMA recovered from the fermentation broth. The reactions were performed with 48.0 mM ctMA solutions in DMSO-d$_6$ and 2 equivalents of H$_2$O and heated to 121 °C. Product distributions were obtained by ^{1}H NMR monitoring with DMSO$_2$ internal standard.

Synthesis and copolymerization of the monounsaturated cyclic diacid CH1DA

Further conversion of Diels–Alder active *tt*MA to TPA and CHDA have been demonstrated in literature.[19,54,55] Here, we show the preparation of novel monounsaturated cyclic diacids and their role on the physical and mechanical properties of Nylon-6,6 when copolymerized with adipic acid and hexamethylenediamine. *tt*MA underwent cycloaddition with ethylene in GVL to form cyclohex-1-ene-1,4-dicarboxylic acid (CH1DA) with >99% yield. Although cyclohex-2-ene-1,4-dicarboxylic acid (CH2DA) is the expected cycloadduct, CH2DA was not detected as it readily isomerizes in GVL likely due to the stabilization resulting from conjugation (Scheme 5).

The synthesized CH1DA was further copolymerized with adipic acid and hexamethylenediamine to demonstrate the potential of this new monomer for tuning the properties of conventional Nylon. To maintain an equimolar ratio between the diacid and diamine, 10 to 25 mol% of adipic acid were replaced by CH1DA (Fig. 8). This range was selected taking into consideration the economic feasibility of using novel chemicals. Gel permeation chromatography (GPC), differential
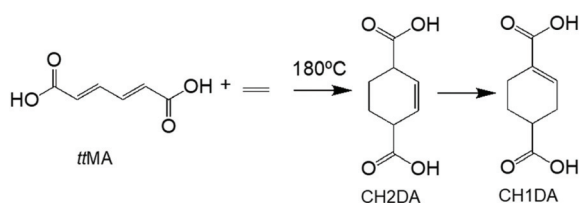
Scheme 5 Reaction between *tt*MA and ethylene to produce monounsaturated cyclic diacid CH1DA.
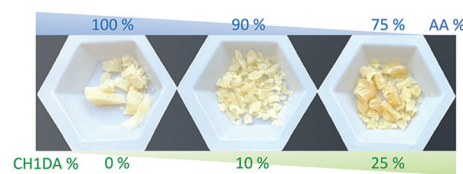

Fig. 8 Copolymerization of adipic acid (AA) and CH1DA with hexamethylene diamine.

Table 5 Properties of polyamides with various molar incorporation of CH1DA[a]

Sample	M_n [kDa]	PDI	T_{melt} [°C]	G' [GPa]	G'' [MPa]	T_g [°C]
PA66	16.5	2.5	261.0	1.32	16.52	73.3
CH1DA-10%	15.8	2.1	250.2	1.65	17.39	75.8
CH1DA-25%	12.4	2.3	232.6	1.65	10.99	80.3

[a] M_n: number-average molecular weight with reference to poly(methyl methacrylate) standards; PDI: polydispersity index; G', G'': storage and loss moduli in the glassy plateau at 0 °C; T_g: glass transition temperature calculated from peak of tan(∂).

scanning calorimetry (DSC), and dynamic mechanical analysis (DMA) were used to characterize these polymers using Nylon-6,6 as a reference (ESI 4–6†). The corresponding results are summarized in Table 5. The addition of the cyclic diacid into Nylon's aliphatic backbone altered its crystallinity due to the defects introduced by CH1DA sequences. This change reduces the polymer's melting temperature from 261 to 233 °C, which facilitates its processing through blow molding. Moreover, introducing a cyclic molecule in the polymer backbone increased the rigidity of polymer chains, thereby increasing the storage modulus and glass transition temperatures. The addition of CH1DA allows control over Nylon-6,6 thermal properties without sacrificing its mechanical properties, as shown in Table 5. Overall, CH1DA offers a renewable alternative to commercially available products such as INVISTA's Dytek diamines with the additional benefit of providing an unsaturated bond. This unsaturation allows for further functionalization to insert properties such as hydrophobicity and flame retardance directly into Nylon's backbone.[28]

Conclusion

A novel solvent-driven, catalyst-free, isomerization of *ct*MA to *tt*MA was demonstrated and investigated mechanistically. The lactonization process that is dominant in aqueous media was overcome in solvent systems combining the polar aprotic solvent DMSO and water.[19] In dry DMSO, MA generates a significant quantity of lactones through an acid-catalyzed pathway analogous to the aqueous system. This reaction is enhanced at higher [*ct*MA] due to MA acting as both the catalyst and reactant. The addition of 1 equivalent of water has the effect of reducing the apparent acidity of the system, thereby

reducing lactonization. Consequently, the S_{ttMA} was increased by 13-fold.

The production of *tt*MA is a relatively slow process, particularly at high [*ct*MA]. This is believed to be due to the formation of a non-reactive MA complex that slow the kinetics. The system is also limited by the reversibility of the system in DMSO/H$_2$O mixtures, which was not previously observed in the aqueous system. Nevertheless, high yields of *tt*MA can be obtained at elevated temperatures in a relatively short period of time due to a shift in the *ct*MA to *tt*MA equilibrium constant favoring *tt*MA (nearly 5 : 1 at 121 °C). Although further increase in temperature would favor isomerization to *tt*MA, it needed to be balanced with the decomposition of DMSO at elevated temperatures.[50]

Continued addition of water sheds light on the role of solvent in both isomerization and lactonization for the aqueous system. Previous work supported by simulations and kinetic measurements indicated that the isomerization of *cc*MA to *ct*MA and the lactonization of *ct*MA to Mlac were unimolecular reactions. However, these reactions were both accompanied by relatively large entropies of activation (−88 and −110 J (mol K)$^{-1}$, respectively).[19] While the involvement of water in the isomerization of *cc*MA is still not definitively shown, it is strongly supported by the increase in k_{obs} with water content and apparent saturation kinetics when D$_2$O was in large excess of MA. Lactonization of *ct*MA, on the other hand, is strongly supported by the dependence of k_{Mlac} on [D$_2$O]. Furthermore, this observed dependence on [D$_2$O] indicates that this transformation is a ternary reaction in which water acts as both a proton donor and a proton acceptor (Scheme 2). In addition to the enhanced lactonization at high [D$_2$O], $k_{ct \rightarrow tt}$ becomes slower while $k_{tt \rightarrow ct}$ remains unchanged; resulting in a shift in the apparent equilibrium constant to favor *ct*MA over *tt*MA. Perhaps this offers an explanation as to why *tt*MA has never been observed to form in aqueous solutions without the presence of a catalyst.

Under optimal conditions (2 equivalents of water, 121 °C), *ct*MA is isomerized to *tt*MA with 88% selectivity, with Mlac and degradation products representing less than 3% of the mixture. The other species in solution are *ct*MA (in equilibrium with *tt*MA) and *cc*MA (in equilibrium with ctMA). In an industrial setting, *cc*MA and *ct*MA would be recovered and recycled, making it a scalable, green, and cost-efficient process.

This advancement in MA isomerization technology will not only allow for the development of biobased commodity chemicals such as TPA, but also for novel unsaturated cyclic molecules such as CH1DA. Incorporation of CH1DA in a polyamide backbone enabled tunable properties that could help with processability of polymers. Further modification of the alkene moiety in this diacid could additionally achieve targeted property enhancement in polyesters and polyamides.

Experimental

cis,cis-muconic acid (*cc*MA), *trans,trans*-muconic acid (*tt*MA), DMSO-d$_6$ (99.96% D), γ-valerolactone (GVL), tetrahydrofuran

(THF), hexamethylenediamine (HMDA), adipic acid (AA), tetramethylsilane and dimethyl sulfone (DMSO$_2$) were purchased from Sigma-Aldrich. Ethylene gas was purchased from Airgas at 99.5% purity. *cis,trans*-Muconic acid (*ct*MA) was prepared by methods previously described in the literature.[41] Extra-dry DMSO-d$_6$ was refluxed over CaH$_2$ and stored over sieves.

For experiments in which strict water-free conditions were required, a mother solution containing *ct*MA and DMSO$_2$ (internal standard) with dried DMSO-d$_6$ was prepared in an inert atmosphere box. Experiments in which the effect of [MA] was investigated utilized 600 μL of the mother solution in J. Young tubes containing additional solid *ct*MA. *ct*MA concentrations were determined by NMR *vs.* DMSO$_2$ internal standard in the mother solution. The tubes were sealed, placed in an Erlenmeyer flask with a thermometer, and heated in a laboratory oven. The experiments at 121 °C were carried out using an aluminum heating block equipped with a thermocouple. Samples were removed from the oven, cooled to room temperature, and analyzed by ^{1}H NMR throughout the duration of the experiment. Experiments that investigated the effect of water were prepared in DMSO-d$_6$ that had not been dried. Instead, aliquots of a mother solution containing *ct*MA and DMSO$_2$ were added to J. Young tubes and H$_2$O was added *via* syringe (<1 μL–100 μL). The water concentration was determined by ^{1}H NMR signal relative to DMSO$_2$ standard. High water concentration experiments (>1 M) utilized D$_2$O to minimize interference with ^{1}H NMR spectra. D$_2$O was added to the mother solution with an electronic micropipette (>100 μL). Dilution of [*ct*MA] was adjusted by addition of solid *ct*MA and was again determined relative to [DMSO$_2$] internal standard.

Cyclohex-1-ene-1,4-dicarboxylic acid (CH1DA) was produced through a Diels–Alder cycloaddition of *tt*MA with 500 psig ethylene in γ-valerolactone at 180 °C for 24 hours in a 50 ml pressurized reactor (Parr 4590 Series). The products in the liquid phase were filtered using a cellulose filter, washed repeatedly with water, and dried overnight in a drying oven. The dried product was then dissolved in DMSO-d$_6$ and characterized using NMR using tetramethylsilane as internal standard.

To prepare the salt for polymerization, adipic acid and CH1DA were added in the molar ratio of $x : (1 - x)$ with $0.75 \leq x \leq 1$ and dissolved in methanol and THF, respectively. The molar equivalent of HMDA was then added to the resulting mixtures and heated to 40 °C. The precipitated salt was filtered, washed and dried overnight in a fume hood. Polymerization was carried out in a Parr reactor charged with the salt and 60 wt% water and pressurized with 100 psig N$_2$. The mixture was heated to an internal temperature of 210 °C, held there for 80 minutes, followed by venting out the N$_2$ and water. The sample was then allowed to polymerize at an internal temperature of 270 °C at atmospheric pressure for 1.5 hours and cooled to room temperature. Molecular weight of copolymers was obtained through gel permeation chromatography (GPC) using EcoSEC GPC system. Polymer samples of around 5 mg were dissolved in 1,1,1,3,3,3-hexafluoroiso-

propanol and compared to poly(methyl methacrylate) standards. Samples were then annealed in an oven for 6 hours at 150 °C. DSC was carried out on the copolymer using TA Q100. Dynamic mechanical analysis was performed using a TA ARES-G2 rheometer.

^{1}H NMR spectra were collected with a Bruker AVIII600 spectrometer, and spectra were analyzed with MestReNova software. Data were plotted with OriginPro 9.1 software.

Conflicts of interest

There are no conflicts to declare.

Acknowledgements

References

1 N. Hernández, R. C. Williams and E. W. Cochran, *Org. Biomol. Chem.*, 2014, **12**, 2834–2849.
2 S. Laurichesse and L. Avérous, *Prog. Polym. Sci.*, 2014, **39**, 1266–1290.
3 R. P. Babu, K. O'Connor and R. Seeram, *Prog. Biomater.*, 2013, **2**, 8.
4 T. Iwata, *Angew. Chem., Int. Ed.*, 2015, **54**, 3210–3215.
5 D. I. Collias, A. M. Harris, V. Nagpal, I. W. Cottrell and M. W. Schultheis, *Ind. Biotechnol.*, 2014, **10**, 91–105.
6 C.-C. Chang, S. K. Green, C. L. Williams, P. J. Dauenhauer and W. Fan, *Green Chem.*, 2014, **16**, 585–588.
7 H. J. Cho, L. Ren, V. Vattipalli, Y.-H. Yeh, N. Gould, B. Xu, R. J. Gorte, R. Lobo, P. J. Dauenhauer, M. Tsapatsis and W. Fan, *ChemCatChem*, 2017, **9**, 398–402.
8 C. L. Williams, C.-C. Chang, P. Do, N. Nikbin, S. Caratzoulas, D. G. Vlachos, R. F. Lobo, W. Fan and P. J. Dauenhauer, *ACS Catal.*, 2012, **2**, 935–939.
9 S. Bérard, C. Vallée and D. Delcroix, *Ind. Eng. Chem. Res.*, 2015, **54**, 7164–7168.
10 T. Pfennig, R. L. Johnson and B. H. Shanks, *Green Chem.*, 2017, **19**, 3263–3271.
11 T. Pfennig, A. Chemburkar, S. Cakolli, M. Neurock and B. H. Shanks, *ACS Sustainable Chem. Eng.*, 2018, **6**, 12855–12864.
12 Y. Xiao, Q. Meng, X. Pan, C. Zhang, Z. Fu and C. Li, *Green Chem.*, 2020, **22**, 4341–4349.
13 R. Y. Rohling, E. Uslamin, B. Zijlstra, I. C. Tranca, I. A. W. Filot, E. J. M. Hensen and E. A. Pidko, *ACS Catal.*, 2018, **8**, 760–769.
14 Y.-T. Cheng, J. Jae, J. Shi, W. Fan and G. W. Huber, *Angew. Chem., Int. Ed.*, 2012, **51**, 1387–1390.
15 C. Li, X. Zhao, A. Wang, G. W. Huber and T. Zhang, *Chem. Rev.*, 2015, **115**, 11559–11624.
16 A. E. Settle, L. Berstis, N. A. Rorrer, Y. Roman-Leshkóv, G. T. Beckham, R. M. Richards and D. R. Vardon, *Green Chem.*, 2017, **19**, 3468–3492.
17 S. Thiyagarajan, H. C. Genuino, J. C. van der Waal, E. de Jong, B. M. Weckhuysen, J. van Haveren, P. C. A. Bruijnincx and D. S. van Es, *Angew. Chem., Int. Ed.*, 2016, **55**, 1368–1371.
18 Y. Hu, Z. Zhao, Y. Liu, G. Li, A. Wang, Y. Cong, T. Zhang, F. Wang and N. Li, *Angew. Chem.*, 2018, **130**, 7017–7021.
19 J. M. Carraher, T. Pfennig, R. G. Rao, B. H. Shanks and J.-P. Tessonnier, *Green Chem.*, 2017, **19**, 3042–3050.
20 Purified Terephthalic Acid Market Size, Share | Industry Report, 2025, https://www.grandviewresearch.com/industry-analysis/purified-terephthalic-acid-market, (accessed June 3, 2020).
21 Purified Terephthalic Acid (PTA) Market, https://www.marketsandmarkets.com/Market-Reports/purified-terephthalic-acid-market-150628286.html, (accessed June 3, 2020).
22 T. Dai, C. Li, L. Li, Z. K. Zhao, B. Zhang, Y. Cong and A. Wang, *Angew. Chem., Int. Ed.*, 2018, **57**, 1808–1812.
23 F. Wang and Z. Tong, *ChemistrySelect*, 2016, **1**, 5538–5541.
24 J. W. Frost and K. M. Draths, Synthesis of adipic acid from biomass-derived carbon sources, US5487987A, 1996.
25 D. R. Vardon, M. A. Franden, C. W. Johnson, E. M. Karp, M. T. Guarnieri, J. G. Linger, M. J. Salm, T. J. Strathmann and G. T. Beckham, *Energy Environ. Sci.*, 2015, **8**, 617–628.
26 K. A. Curran, J. M. Leavitt, A. S. Karim and H. S. Alper, *Metab. Eng.*, 2013, **15**, 55–66.
27 M. Suástegui and Z. Shao, *J. Ind. Microbiol. Biotechnol.*, 2016, **43**, 1611–1624.
28 M. Suastegui, J. E. Matthiesen, J. M. Carraher, N. Hernandez, N. Rodriguez Quiroz, A. Okerlund, E. W. Cochran, Z. Shao and J.-P. Tessonnier, *Angew. Chem., Int. Ed.*, 2016, **55**, 2368–2373.
29 B. H. Shanks and P. L. Keeling, *Green Chem.*, 2017, **19**, 3177–3185.
30 B. H. Shanks and L. J. Broadbelt, *ChemSusChem*, 2019, **12**, 2970–2975.
31 X. Zhou, Z. J. Brentzel, G. A. Kraus, P. L. Keeling, J. A. Dumesic, B. H. Shanks and L. J. Broadbelt, *ACS Sustainable Chem. Eng.*, 2019, **7**, 2414–2428.
32 S. Capelli, D. Motta, C. Evangelisti, N. Dimitratos, L. Prati, C. Pirola and A. Villa, *ChemCatChem*, 2019, **11**, 3075–3084.
33 A. Rosengart, S. Capelli, C. Pirola, A. Citterio, C. L. Bianchi, L. Prati and A. Villa, *Chem. Eng. Trans.*, 2017, **57**, 931–936.
34 W. Niu, K. M. Draths and J. W. Frost, *Biotechnol. Prog.*, 2002, **18**, 201–211.
35 C. Müller, *et al.*, *Method for producing hexamethylenediamine*, WO2015086819A1, 2015.
36 D. R. Vardon, N. A. Rorrer, D. Salvachúa, A. E. Settle, C. W. Johnson, M. J. Menart, N. S. Cleveland, P. N. Ciesielski, K. X. Steirer, J. R. Dorgan and G. T. Beckham, *Green Chem.*, 2016, **18**, 3397–3413.

37 R. Beerthuis, G. Rothenberg and N. R. Shiju, *Green Chem.*, 2015, **17**, 1341–1361.

38 L. Coudray, V. Bui, J. W. Frost and D. Schweitzer, Process for Preparing Caprolactam and Polyamides Therefrom, US20130085255A1, 2013.

39 R. Lu, F. Lu, J. Chen, W. Yu, Q. Huang, J. Zhang and J. Xu, *Angew. Chem., Int. Ed.*, 2016, **55**, 249–253.

40 J. W. Frost, A. Miermont, D. Schweitzer and V. Bui, Preparation of trans, trans muconic acid and trans, trans muconates, US8426639, 2013.

41 J. E. Matthiesen, J. M. Carraher, M. Vasiliu, D. A. Dixon and J.-P. Tessonnier, *ACS Sustainable Chem. Eng.*, 2016, **4**, 3575–3585.

42 J. E. Matthiesen, M. Suástegui, Y. Wu, M. Viswanathan, Y. Qu, M. Cao, N. Rodriguez-Quiroz, A. Okerlund, G. Kraus, D. R. Raman, Z. Shao and J.-P. Tessonnier, *ACS Sustainable Chem. Eng.*, 2016, **4**, 7098–7109.

43 J.-P. Tessonnier, J. E. Matthiesen, T. Pfennig, B. H. Shanks and J. M. Carraher, Electrochemical isomerization of muconic acid, US10465043B2, 2016.

44 J.-P. Tessonnier, J. M. Carraher, T. Pfennig and B. H. Shanks, Isomerization of muconic acid, US9957218B2, 2016.

45 J. K. Ogunjobi, T. J. Farmer, C. R. McElroy, S. W. Breeden, D. J. Macquarrie, D. Thornthwaite and J. H. Clark, *ACS Sustainable Chem. Eng.*, 2019, **7**, 8183–8194.

46 I. Khalil, G. Quintens, T. Junkers and M. Dusselier, *Green Chem.*, 2020, **22**, 1517–1541.

47 V. Bui, M. K. Lau, D. MacRae and D. Schweitzer, Methods for producing isomers of muconic acid and muconate salts, US8809583B2, 2014.

48 J. W. Frost, A. Miermont, D. Schweitzer and B. Vu, Preparation of trans, trans muconic acid and trans, trans muconates, WO2010148049A2, 2010.

49 A. E. Settle, L. Berstis, S. Zhang, N. A. Rorrer, H. Hu, R. M. Richards, G. T. Beckham, M. F. Crowley and D. R. Vardon, *ChemSusChem*, 2018, **11**, 1768–1780.

50 F. P. Byrne, S. Jin, G. Paggiola, T. H. M. Petchey, J. H. Clark, T. J. Farmer, A. J. Hunt, C. R. McElroy and J. Sherwood, *Sustainable Chem. Processes*, 2016, **4**, 7.

51 M. Martí, L. Molina, C. Alemán and E. Armelin, *ACS Sustainable Chem. Eng.*, 2013, **1**, 1609–1618.

52 J. A. Elvidge, R. P. Linstead, P. Sims and B. A. Orkin, *J. Chem. Soc.*, 1950, 2235.

53 D. M. Alonso, J. M. R. Gallo, M. A. Mellmer, S. G. Wettstein and J. A. Dumesic, *Catal. Sci. Technol.*, 2013, **3**, 927–931.

54 M. J. Burk, R. E. Osterhout and J. Sun, Semi-synthetic terephthalic acid via microorganisms that produce muconic acid, US9562241, 2014.

55 V. Bui, J. W. Frost, D. A. Wicks, D. Schweitzer and A. Miermont, Cyclohexane 1,4 carboxylates, US8367859, 2013.